

See discussions, stats, and author profiles for this publication at: <https://www.researchgate.net/publication/257209370>

# New high pressure vapor–liquid equilibrium data and density predictions for carbon dioxide + ethyl acetate system

ARTICLE *in* FLUID PHASE EQUILIBRIA · JULY 2012

Impact Factor: 2.2 · DOI: 10.1016/j.fluid.2012.03.028

---

CITATIONS

10

---

READS

53

3 AUTHORS, INCLUDING:



Dan Geană

Polytechnic University of Bucharest

138 PUBLICATIONS 744 CITATIONS

SEE PROFILE

# New High Pressure Vapor–Liquid Equilibrium and Density Predictions for the Carbon Dioxide + Ethanol System

Sergiu Sima, Viorel Feroiu,\* and Dan Geană

Department of Applied Physical Chemistry and Electrochemistry, “Politehnica” University Bucharest, 1-7 Polizu Street, 011061, S1, Bucharest, Romania

**ABSTRACT:** Vapor–liquid equilibria (VLE) data at (333.2, 343.2, 363.2, and 373.2) K and pressures between (1.1 and 14.1) MPa and critical data (pressure–temperature–composition) at pressures between (9.1 and 13.9) MPa for the carbon dioxide + ethanol system are reported. The experimental method used in this work was a static analytical method with liquid phase sampling using a rapid online sampler injector (ROLSI) coupled to a gas chromatograph (GC) for analysis. Measured VLE data and literature data for carbon dioxide + ethanol system were modeled with a general cubic equation of state (GEOS) using classical van der Waals (two-parameter conventional mixing rule, 2PCMR) mixing rules. A single set of interaction parameters, representing the critical pressure maximum (CPM) well, was used in this work to represent the new VLE data and critical points and to predict the densities of the mixtures in a wide range of temperature, pressure, and composition. The calculation results were compared to the new data reported in this work and to available literature density data. The results show a satisfactory agreement between the model and the experimental data.

## ■ INTRODUCTION

Supercritical fluid (SFC) processes are merging as important alternative to conventional methods in many fields, such as extraction, particle micronization, material processing, chromatography, or crystallization/purification.<sup>1</sup> Equilibrium and volumetric properties of binary mixtures containing organic solvent and SFCs (especially carbon dioxide) play a fundamental role in determining the success of many of these applications.

High-pressure vapor–liquid equilibrium (VLE) measurements of carbon dioxide + alcohol systems are of interest due to their importance in the supercritical extraction of thermal labile compounds, dehydration of alcohols using supercritical carbon dioxide, and extraction of natural products using near critical solvents.<sup>2</sup>

The low molecular weight alcohols are among the most important compounds in separation processes. They are often used as entrainers to control the polarity of a SFC solvent in extraction applications and are also used as modifiers in SFC chromatography. Carbon dioxide has shown to be the most important SFC for these processes, because it is cheap, nontoxic, and nonflammable and has a low critical temperature of 304.25 K.

The carbon dioxide + ethanol mixture is very important industrially, and the system has received much attention. A complete list of references of the carbon dioxide + ethanol system is covered in our previous paper<sup>3</sup> and will be not repeated in this work. We recorded in our VLE database available experimental data. The goals of this work were to add new experimental VLE data and critical points measured using a rapid online sampler injector (ROLSI)<sup>4</sup> and to represent the global phase behavior and densities of carbon dioxide + ethanol system with a simple cubic equation of state (EOS) model, based on a single set of interaction parameters.

Therefore, in this work we made new VLE measurements using a static–analytical method, in a high-pressure visual cell with variable volume, for carbon dioxide + ethanol. New critical

points (pressure–temperature–composition) were also measured in the same visual cell. Due to the ROLSIs<sup>4</sup> coupled to a gas chromatograph (GC) for analysis used in this work, we consider that the new measured data sets are of better quality than those previously reported in the literature.

In our previous paper,<sup>3</sup> the global phase behavior of the carbon dioxide + ethanol system was modeled with the cubic general equation of state (GEOS),<sup>5–8</sup> coupled with classical van der Waals mixing rules (two-parameter conventional mixing rule, 2PCMR). This cubic equation is a generalized form with four parameters for all cubic equations of state with two, three, and four parameters.<sup>7</sup>

A single set of interaction parameters, representing well the critical pressure maximum (CPM) was used to model the global phase behavior of the carbon dioxide + ethanol system.<sup>3</sup> The same set of parameters is used in this work to represent the new VLE data and critical points and to predict the densities of the mixtures in a wide range of temperature, pressure, and composition. The calculation results were compared to the new data reported in this work and to available literature density data.

## ■ EXPERIMENTAL SECTION

**Materials.** Carbon dioxide (mass fraction purity >0.997) was provided by Linde Gaz Romania, and ethanol (mass fraction purity >0.998) was a Sigma product. The chemicals were used without further purification, except for the careful degassing of ethanol. Gas chromatographic analysis of ethanol gave a mole fraction purity of >0.999.

**Special Issue:** Kenneth N. Marsh Festschrift

**Received:** August 17, 2011

**Accepted:** October 31, 2011

**Published:** November 10, 2011

**Apparatus and Procedure.** A detailed description of the experimental apparatus was presented in earlier papers.<sup>9,10</sup> The apparatus used in this work is based on a high-pressure visual cell with variable volume, to which a ROLSI<sup>4</sup> was added and coupled with a gas chromatograph (GC). The ROLSI is connected by a capillary to the equilibrium cell. A heating resistance is used to heat the expansion chamber of the sampler injector to have liquid samples vaporized rapidly. The transferring line between ROLSI and the GC is heated by means of a linear resistor coupled to a Armines/CEP/TEP regulator. The GC (Perichrom) uses a thermal conductivity detector, TCD, and a 30 m long and 0.530 mm diameter column HP-Plot/Q. The GC carrier gas is helium at a flow rate of 30 mL · min<sup>-1</sup>. The apparatus was completed with a syringe pump Teledyne ISCO model 500D.

The procedure is similar to that in our previous work.<sup>9–15</sup> The entire internal loop of the apparatus including the equilibrium cell was rinsed several times with carbon dioxide. Then, the equilibrium cell was evacuated with a vacuum pump. The cell was charged with alcohol, which was degassed by using a vacuum pump and vigorously stirring. The lighter component (in this case CO<sub>2</sub>) is introduced with the syringe pump into equilibrium cell to set the pressure to the desired value. Then the cell was heated to the experimental temperature. To facilitate the approach to an equilibrium state, the mixture in the cell was stirred for a few hours. Then the stirrer was switched off, and about 1 h was allowed to pass until the coexisting phases were completely separated. Samples of liquid phase are withdrawn by ROLSI and analyzed with GC. At the equilibrium temperature and pressure, we normally analyzed at least six samples of the liquid phase to check the repeatability. The sample sizes being very small, the equilibrium pressure in the cell remains constant.

The calibration of the TCD for CO<sub>2</sub> and ethanol is done by injecting (using gas chromatographic syringes) known amounts of each component. Calibration data are fitted to quadratic polynomials to obtain the mole number of the component versus chromatographic area. The correlation coefficients of the GC calibration curves were 0.999 for carbon dioxide and 0.997 for ethanol.

We estimate the uncertainties in our measurements to be within ± 0.1 K for temperature and to be better than ± 0.01 MPa for pressure from calibration with a precision hydraulic dead-weight tester (model 580C, DH-Budenberg SA, Aubervilliers, France).

The critical points were obtained in this work following the procedure of Scheidgen.<sup>16</sup> At a fixed temperature (for example 373 K), the pressure in the cell was increased by introducing CO<sub>2</sub> with the syringe pump. The transition from heterogeneous (two phases) to the homogeneous range is visually observed. Then, by slowly cooling (1 to 3 K) the pressure in the cell decreases, and the inverse transition from homogeneous to heterogeneous range can be observed. The temperature and the pressure of the opalescence point are considered as critical data points. The composition of the critical point is obtained by sampling from the homogeneous mixture. The procedure is then repeated by introducing new amounts of CO<sub>2</sub> and slowly cooling.

## MODELING

The modeling of phase behavior of this system was made with the cubic GEOS equation,<sup>5–8</sup> coupled with classical van der Waals mixing rules (2PCMR).

**Table 1. Critical Data<sup>17</sup> and GEOS Parameters for Carbon Dioxide and Ethanol<sup>3</sup>**

component	$T_c$	$P_c$	$V_c$	$\alpha_c$	$m$
	K	MPa	cm <sup>3</sup> · mol <sup>-1</sup>		
CO <sub>2</sub>	304.1	73.8	93.9	7.0517	0.3146
C <sub>2</sub> H <sub>5</sub> OH	513.9	61.4	167.1	9.3121	0.6146

The general cubic equation of state (GEOS) has the form:

$$P = \frac{RT}{V-b} - \frac{a(T)}{(V-d)^2 + c} \quad (1)$$

The four parameters  $a$ ,  $b$ ,  $c$ , and  $d$  for a pure component are expressed by:<sup>7</sup>

$$\begin{aligned} a(T) &= a_c \beta(T_r); & a_c &= \Omega_a \frac{R^2 T_c^2}{P_c}; & b &= \Omega_b \frac{RT_c}{P_c}; \\ c &= \Omega_c \frac{R^2 T_c^2}{P_c^2}; & d &= \Omega_d \frac{RT_c}{P_c} \end{aligned} \quad (2)$$

The temperature function used is:

$$\beta(T_r) = T_r^{-m} \quad (3)$$

with the reduced temperature  $T_r = T/T_c$ .

The expressions of the parameters  $\Omega_a$ ,  $\Omega_b$ ,  $\Omega_c$ , and  $\Omega_d$  are:

$$\begin{aligned} \Omega_a &= (1-B)^3; & \Omega_b &= Z_c - B; \\ \Omega_c &= (1-B)^2(B-0.25); & \Omega_d &= Z_c - 0.5(1-B) \end{aligned} \quad (4)$$

$$B = \frac{1+m}{\alpha_c + m} \quad \alpha_c = \text{Riedel's criterion} \quad (5)$$

As observed, the  $a$ ,  $b$ ,  $c$ , and  $d$  coefficients of the cubic GEOS equation are finally functions of critical data ( $T_c$ ,  $P_c$ , and  $V_c$ ),  $m$  and  $\alpha_c$  parameters.

The above eqs 4 and 5 are obtained by setting four critical conditions in reduced variables:

$$P_r = 1; \quad V_r = 1; \quad T_r = 1 \quad (6a)$$

$$\left( \frac{\partial P_r}{\partial V_r} \right)_{T_r} = 0; \quad V_r = 1; \quad T_r = 1 \quad (6b)$$

$$\left( \frac{\partial^2 P_r}{\partial V_r^2} \right)_{T_r} = 0; \quad V_r = 1; \quad T_r = 1 \quad (6c)$$

$$\alpha_c = \left( \frac{\partial P_r}{\partial T_r} \right)_{V_r}; \quad V_r = 1; \quad T_r = 1 \quad (6d)$$

As pointed out previously,<sup>7</sup> the cubic GEOS equation is a general form for all cubic equations of state with two, three, and four parameters. This is the meaning of the statement cubic “general equation of state” used for GEOS.

**Table 2.** Mole Fractions of Component 1 in the Liquid Phase,  $X_1$ , at Various Pressures,  $P$ , and Temperatures,  $T$ , for the Binary System Carbon Dioxide (1) + Ethanol (2)<sup>a</sup>

$X_1$	$T/K$	$P/\text{MPa}$
0.1133	333.2	2.15
0.1748	333.2	3.28
0.2127	333.2	4.09
0.3317	333.2	6.06
0.3870	333.2	6.83
0.4303	333.2	7.59
0.5004	333.2	8.60
0.6890	333.2	10.50
0.0790	343.2	1.44
0.0970	343.2	1.84
0.1470	343.2	2.93
0.2010	343.2	4.08
0.2650	343.2	5.15
0.3090	343.2	6.20
0.3790	343.2	7.30
0.4290	343.2	8.27
0.4880	343.2	9.35
0.0598	363.2	1.12
0.1013	363.2	1.97
0.1400	363.2	3.18
0.2000	363.2	4.63
0.2570	363.2	6.01
0.2727	363.2	6.27
0.3426	363.2	7.82
0.3930	363.2	8.97
0.4507	363.2	10.04
0.4641	363.2	10.21
0.4980	363.2	11.05
0.5554	363.2	12.12
0.6850	363.2	13.75
0.7700	363.2	14.15
0.1315	373.2	3.40
0.2268	373.2	5.72
0.3010	373.2	7.41
0.3608	373.2	8.89
0.5468	373.2	12.36

<sup>a</sup>  $u(T) = 0.1$  K,  $u(P) = 0.01$  MPa, and  $u(X_1) = 0.0005$ .

For example, to obtain the parameters of the Soave–Redlich–Kwong (SRK) equation of state from the eqs 2 to 5 we set the following restrictions:  $\Omega_c = -(\Omega_b/2)^2$  and  $\Omega_d = -\Omega_b/2$ . It follows:

$$\Omega_c = (1 - B)^2(B - 0.25) = -(Z_c - B)^2/4 \quad (7)$$

$$\Omega_d = Z_c - 0.5(1 - B) = -(Z_c - B)/2 \quad (8)$$

It results in  $Z_c(\text{SRK}) = 1/3$ , and the relation for  $B(\text{SRK})$  is:

$$B = 0.25 - \frac{1}{36} \left( \frac{1 - 3B}{1 - B} \right)^2 \quad (9)$$

Solving iteratively this equation gives  $B(\text{SRK}) = 0.2467$ , and correspondingly:  $\Omega_a(\text{SRK}) = (1 - B)^3 = 0.42748$  and  $\Omega_a(\text{SRK}) = Z_c - B = 0.08664$ .

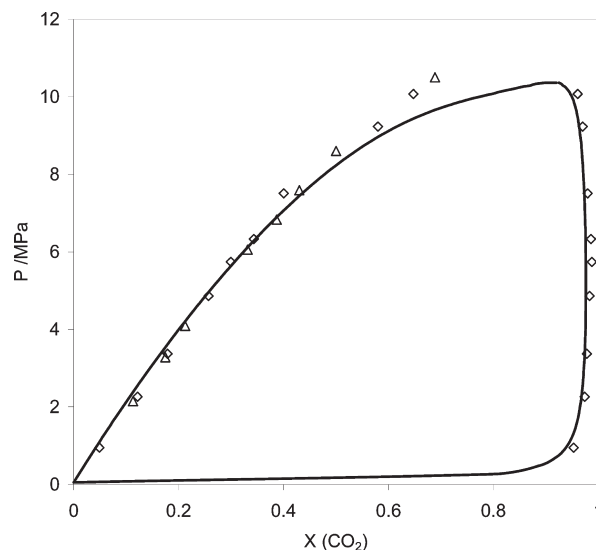


**Figure 1.** Comparison of measured and literature data for the carbon dioxide (1) + ethanol (2) system at  $T = 333.2$  K:  $\Delta$ , this work;  $\diamond$ , literature;<sup>3</sup> —, GEOS/2PCMR prediction.

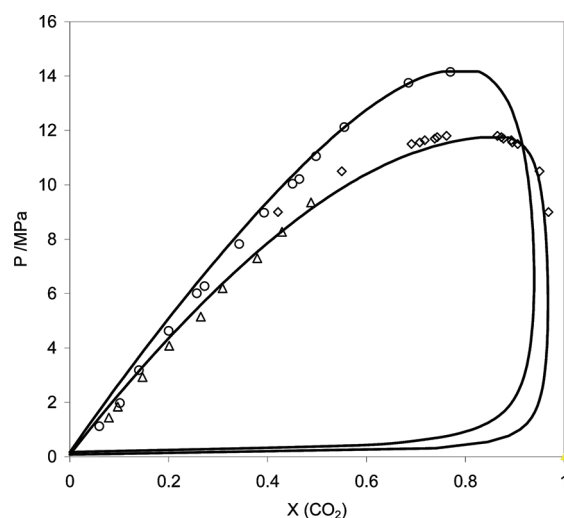


**Figure 2.** Comparison of measured and literature data for the carbon dioxide (1) + ethanol (2) system at  $T = 343.2$  K and  $T = 363.2$  K:  $\Delta$ , this work (343.2 K);  $\circ$ , this work (363.2 K);  $\diamond$ , literature (343.15 K);<sup>23</sup> —, GEOS/2PCMR prediction.

For Peng–Robinson (PR) equation of state we set the restrictions:  $\Omega_c = -2(\Omega_b)^2$  and  $\Omega_d = -\Omega_b$ . It results in:

$$B = 0.25 - \frac{1}{8} \left( \frac{1 - 3B}{1 - B} \right)^2; \quad Z_c = \frac{1 + B}{4} \quad (10)$$

giving  $B(\text{PR}) = 0.2296$  and  $Z_c(\text{PR}) = 0.3074$ .

In this work, the coefficients  $a$ ,  $b$ ,  $c$ , and  $d$  were obtained for mixtures using the classical van der Waals mixing rules:

$$\begin{aligned} a &= \sum_i \sum_j X_i X_j c_{ij}; & b &= \sum_i \sum_j X_i X_j b_{ij}; \\ c &= \sum_i \sum_j X_i X_j c_{ij}; & d &= \sum_i X_i d_i \end{aligned} \quad (11)$$

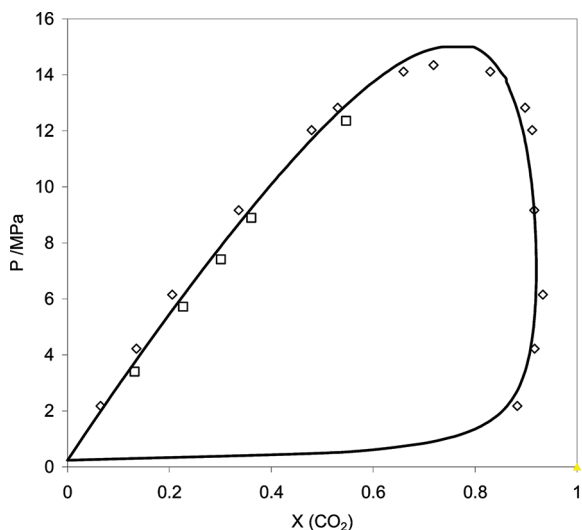


**Figure 3.** Comparison of measured and literature data for the carbon dioxide (1) + ethanol (2) system at  $T = 373.2$  K:  $\square$ , this work;  $\diamond$ , literature;<sup>24</sup> —, GEOS/2PCMR prediction.

**Table 3. Measured Critical Data for the System Carbon Dioxide (1) + Ethanol (2)<sup>a</sup>**

$P_c$ /MPa	$T_c$ /K	$X_{1c}$
13.86	364.2	0.8315
13.70	361.65	0.8380
13.11	355.05	0.8401
12.54	348.65	0.8409
12.00	342.65	0.8420
11.17	335.65	0.8507
10.60	332.2	0.9010
10.45	330.2	0.8920
9.84	325.7	0.9080
9.10	321.2	0.9310

<sup>a</sup>  $u(T_c) = 0.5$  K,  $u(P_c) = 0.05$  MPa, and  $u(X_{1c}) = 0.0005$ .

$$a_{ij} = (a_i a_j)^{1/2} (1 - k_{ij}) \quad b_{ij} = \frac{b_i + b_j}{2} (1 - l_{ij})$$

$$c_{ij} = \pm (c_i c_j)^{1/2}$$

(with “+” for  $c_i, c_j > 0$  and “−” for  $c_i, c_j < 0$ ) (12)

Generally, negative values are common for the  $c$  parameter of pure components.

The GEOS parameters  $m$  and  $\alpha_c$  were estimated by constraining the EOS to reproduce the experimental vapor pressure and liquid volume on the saturation curve between the triple point and the critical point. The values of critical data and GEOS parameters of the pure components are given in Table 1.<sup>17,3</sup>

The binary interaction parameters,  $k_{12}$  and  $l_{12}$ , were estimated in our previous paper,<sup>3</sup> to represent the CPM well and to decrease the temperature of the UCEP at lower temperature ( $\sim 270$  K). The carbon dioxide + ethanol system is a Type I phase behavior, according to the classification of van Konynenburg and Scott.<sup>18</sup> The region of the Type I (II) phase behavior can be obtained by tracing the tricritical and double critical end point boundary curves in the  $k_{12}$ – $l_{12}$  global phase diagram of Polishuk et al.<sup>19</sup> These types of phase behavior are located on the left side

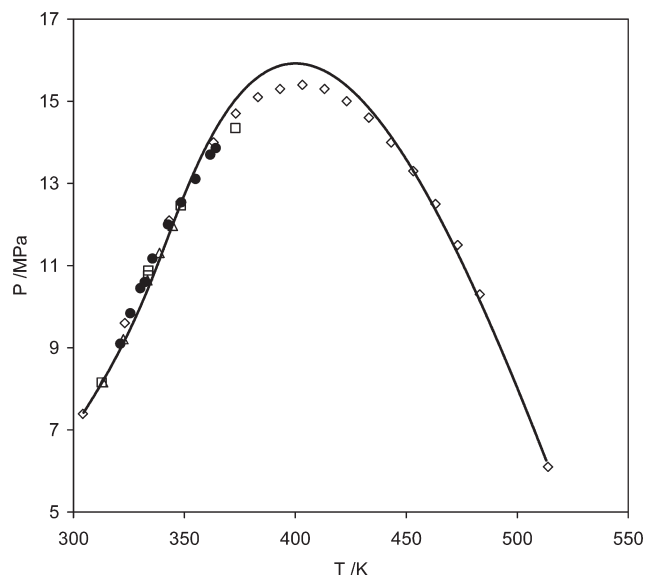


**Figure 4.**  $P$ – $T$  fluid phase diagram of the carbon dioxide + ethanol system. Experimental critical curve:  $\bullet$ , critical points measured in this work;  $\diamond$ , literature;<sup>25</sup>  $\square$ , literature;<sup>24</sup>  $\triangle$ , literature.<sup>26</sup> Calculation: —, GEOS/2PCMR prediction.

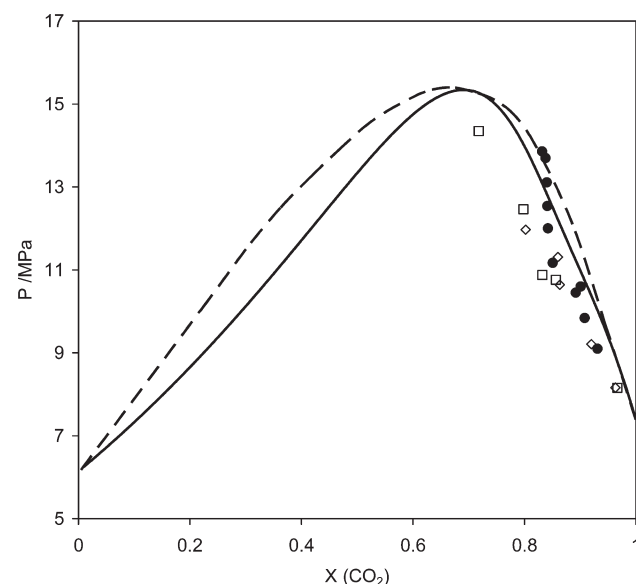


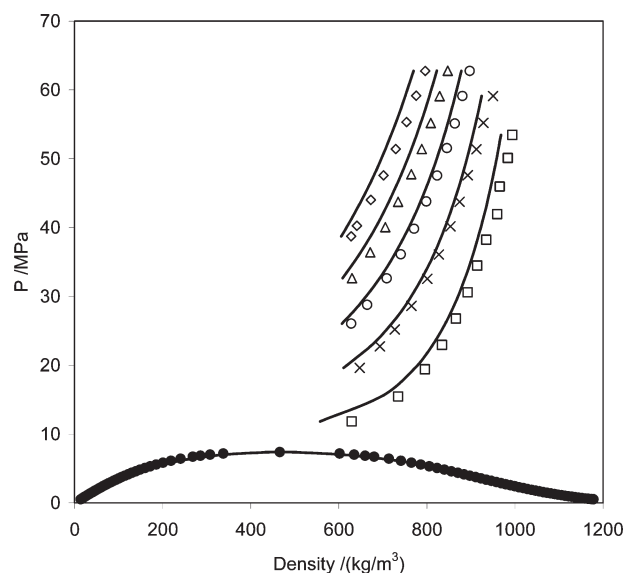
**Figure 5.** Critical pressure of binary mixtures carbon dioxide + ethanol. Experimental critical curve:  $\bullet$ , critical points measured in this work;  $\diamond$ , literature;<sup>26</sup>  $\square$ , literature;<sup>24</sup> - - - critical curve, literature;<sup>27</sup> —, GEOS/2PCMR prediction.

of the tricritical boundary. The values of the interaction binary parameters ( $k_{12}$  and  $l_{12}$ ) fulfilling these requirements are  $k_{12} = 0.06$ ,  $l_{12} = -0.01$ . This set of interaction parameters was used in this work to predict the topology of phase behavior, the critical, the bubble-, and dew-point lines, and the mixture densities.

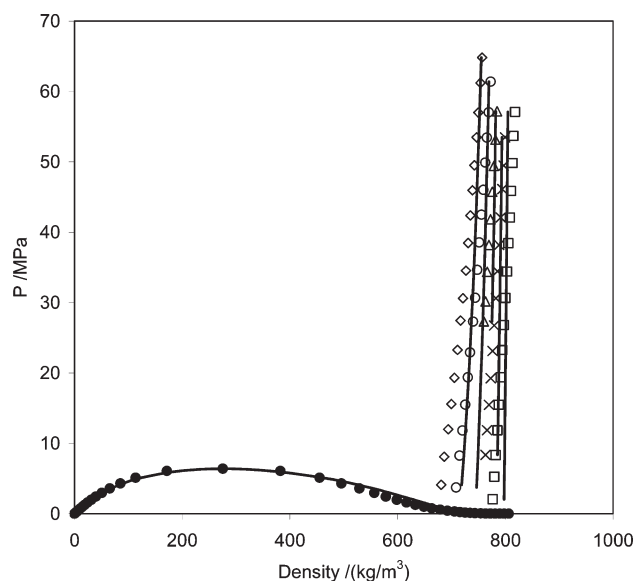
The calculations were made using the software package PHEQ, developed in our laboratory.<sup>20</sup> The critical curves were calculated using the method proposed by Heidemann and Khalil,<sup>21</sup> with numerical derivatives given by Stockfleth and Dohrn.<sup>22</sup>

Table 4. Average Absolute Deviations in Compressed Liquid Densities of the Carbon Dioxide + Ethanol System

composition ( $X_{\text{CO}_2}$ )	min-max $P/\text{MPa}$	min-max $T/\text{K}$	no. data points	AAD% density	lit.
1.0000	11.83–62.78	323.15–423.15	52	2.7	28
0.0000	2.04–64.81	323.15–423.15	72	1.6	28
0.90404	10.23–64.69	323.15–423.15	58	2.3	28
0.80722	9.56–61.26	323.15–423.15	60	4.9	28
0.70951	9.56–57.21	323.15–423.15	54	4.1	28
0.51143	8.02–57.45	323.15–423.15	69	9.9	28
0.23170	7.92–25.16	312.95–362.56	103	4.7	29
0.40760	7.99–25.20	313.16–362.79	91	7.5	29
0.55690	8.32–25.17	313.16–362.78	91	14.4	29
0.77030	11.0–24.0	313.16–323.12	16	10.7	29



**Figure 6.** Phase equilibrium diagram (pressure–density) for carbon dioxide. Experimental data:<sup>28</sup> ●, saturated liquid densities; □,  $T = 323$  K; ×,  $T = 348$  K; ○,  $T = 373$  K; △,  $T = 398$  K; ◇,  $T = 423$  K. Calculation: —, GEOS/2PCMR prediction.



**Figure 7.** Phase equilibrium diagram (pressure–density) for ethanol. Experimental data:<sup>28</sup> ●, saturated liquid densities; □,  $T = 323$  K; ×,  $T = 348$  K; △,  $T = 373$  K; ○,  $T = 398$  K; ◇,  $T = 423$  K; Calculation: —, GEOS/2PCMR prediction.

## RESULTS AND DISCUSSION

The equilibrium compositions for the carbon dioxide + ethanol binary system were measured at (333.2, 343.2, 363.2, and 373.2) K and pressures between (1.1 and 14.1) MPa, and the results are given in Table 2. The values are typically averages of five or six sample measurements. For the VLE measurements, the uncertainty of the mole fraction in the liquid phase is typically 0.0005. GEOS calculations with the single set of parameters ( $k_{12} = 0.06$ ,  $l_{12} = -0.01$ ) were done for the new experimental data of this work and for data sets from literature at temperatures between (333 and 373) K.

Figure 1 shows a comparison of our data (symbols) from this work with our previous published data at 333.2 K, measured using manually operated valves,<sup>3</sup> and with the prediction results by GEOS equation (line). As can be seen, both sets of data are in good agreement and are satisfactorily represented by the predicted curve with the GEOS equation. Other isotherms (343 K, 363 K, and 373 K) comparing the prediction results with experimental data of this work are illustrated in Figures 2 and 3. At 343 K and 373 K, literature data of Lim et al.<sup>23</sup> and Galicia-Luna et al.<sup>24</sup>

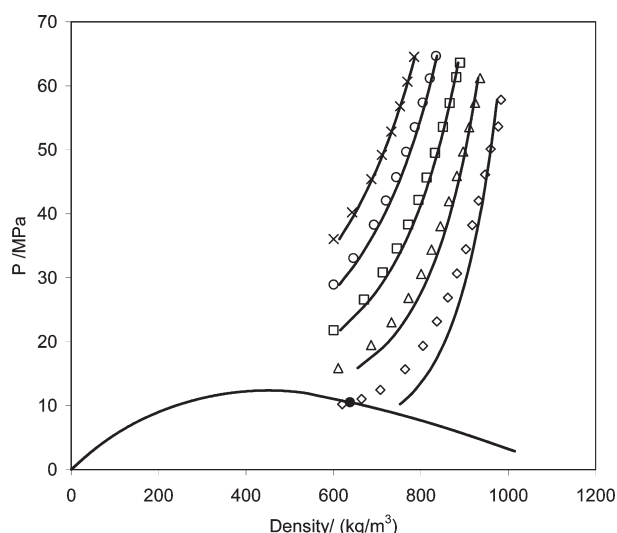
are given too. Taking into account the semipredictive approach used in our previous work,<sup>3</sup> the single set of interaction parameters leads to a satisfactory prediction of VLE for the carbon dioxide + ethanol system.

The critical properties ( $P_c$ ,  $T_c$ ,  $X_{1c}$ ) for the carbon dioxide + ethanol binary system, measured in this work at pressures between (9.1 and 13.9) MPa, are given in Table 3. The compositions of critical points were obtained with the same accuracy as that for VLE by gas chromatograph analysis. The accuracy of critical temperature was  $\pm 0.5$  K and of critical pressure was  $\pm 0.05$  MPa from visual observation through the sapphire windows of the cell.

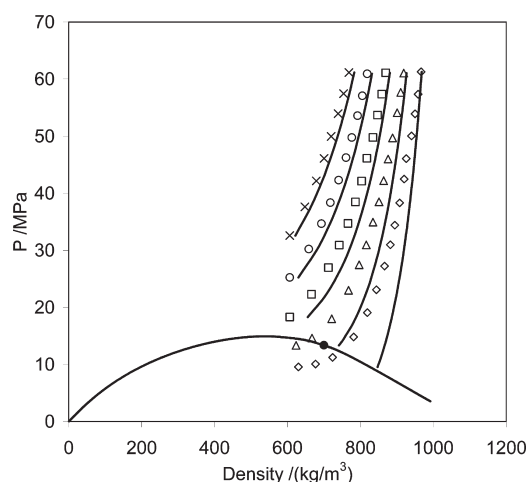
Figure 4 shows a comparison of critical  $P_c$ – $T_c$  data (symbols) from this work with literature published data.<sup>24–26</sup> In this figure we have illustrated also the prediction with GEOS/2PCMR for  $k_{12} = 0.06$  and  $l_{12} = -0.01$ . As can be seen, all sets of data are in good agreement and are well-represented by the predicted curve with the GEOS equation. It can be observed that the CPM is a little overestimated.

Figure 5 shows the variation of the critical pressure with the composition (mole fraction of carbon dioxide) for the measured





**Figure 8.** Phase equilibrium diagram (pressure–density) at constant composition ( $X_1 = 0.90404$ ) for the carbon dioxide (1) + ethanol (2) system. Experimental data:<sup>28</sup>  $\diamond$ ,  $T = 323$  K;  $\triangle$ ,  $T = 348$  K;  $\square$ ,  $T = 373$  K;  $\circ$ ,  $T = 398$  K;  $\times$ ,  $T = 423$  K. Calculation:  $\bullet$ , predicted critical point; —, GEOS/2PCMR prediction.



**Figure 9.** Phase equilibrium diagram (pressure–density) at constant composition ( $X_1 = 0.80722$ ) for the carbon dioxide (1) + ethanol (2) system. Experimental data:<sup>28</sup>  $\diamond$ ,  $T = 323$  K;  $\triangle$ ,  $T = 348$  K;  $\square$ ,  $T = 373$  K;  $\circ$ ,  $T = 398$  K;  $\times$ ,  $T = 423$  K. Calculation:  $\bullet$ , predicted critical point; —, GEOS/2PCMR prediction.

data in this work and available data in the literature.<sup>24,26</sup> As can be observed from this figure, all data are in a limited composition range, and there are significant deviations among the data from different sources. Two calculated curves have been included in the figure, one calculated by the method of Li<sup>27</sup> and the other by GEOS. The existing data are better reproduced by the GEOS equation.

Based on the capability of GEOS equation to predict reasonably well the VLE and the critical behavior of carbon dioxide + ethanol system, we try to predict also the densities of this system in a wide range of temperature, pressure, and composition. In a previous paper we tested the capacity of cubic EOSs to predict simultaneously the volumetric and thermodynamic properties and VLE for pure refrigerants and refrigerant mixtures.<sup>8</sup> The

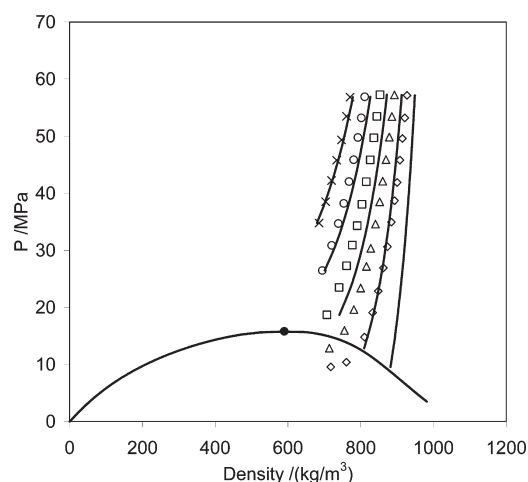


**Figure 10.** Phase equilibrium diagram (pressure–density) at constant composition ( $X_1 = 0.70951$ ) for the carbon dioxide (1) + ethanol (2) system. Experimental data:<sup>28</sup>  $\diamond$ ,  $T = 323$  K;  $\triangle$ ,  $T = 348$  K;  $\square$ ,  $T = 373$  K;  $\circ$ ,  $T = 398$  K;  $\times$ ,  $T = 423$  K. Calculation:  $\bullet$ , predicted critical point; —, GEOS/2PCMR prediction.

GEOS equation has compared favorably to other cubic equation in literature, resting simple enough for applications. Therefore, we used the GEOS equation with the same set of interaction parameters ( $k_{12} = 0.06$ ,  $l_{12} = -0.01$ ) to predict the compressed liquid densities of the carbon dioxide + ethanol mixture at temperatures between (312 and 423) K and pressures in the range (8 to 65) MPa. The predictions are compared with the experimental data of Pohler and Kiran<sup>28</sup> and Zuniga-Moreno and Galicia-Luna.<sup>29</sup>

Table 4 presents the ranges in temperature, pressure, and composition as well as the number of data points used in this work. Data refer to pure components (carbon dioxide and ethanol) and eight constant composition mixtures. The densities of pure component and mixtures given in Table 4 were calculated from the cubic GEOS equation. The calculation results are presented as AAD% density (the average absolute deviations of calculated densities). As can be seen, the pure component densities are well-represented by the GEOS equation (AAD < 3 %). The AAD for the mixtures are between 2.3 % and 14.4 % depending on pressure and temperature ranges. Unfortunately, the averages cannot show the details of deviations between the experimental data and the calculations. Therefore, we illustrate in the following figures the deviations between experimental data and calculated densities in different ranges of temperature, pressure, and composition.

In Figures 6 and 7, the pressure–density curves predicted with GEOS are presented for the pure components together with the isotherms (experimental and calculated values). The calculations are in good agreement with the experimental data for both components. As can be seen, ethanol has a relatively low compressibility, displayed by the steep increase in pressure with changes in the density of the fluid.

Figures 8 to 12 show the pressure–density diagrams for mixtures at constant composition. The phase boundary lines (isopleths) predicted with GEOS are presented together with the isotherms (experimental and calculated values). The phase boundary lines enclose the region on these diagrams for which more than one phase is present in the system. The critical point divides the phase boundary line in two branches, the dew line at low densities and the bubble line at high densities.

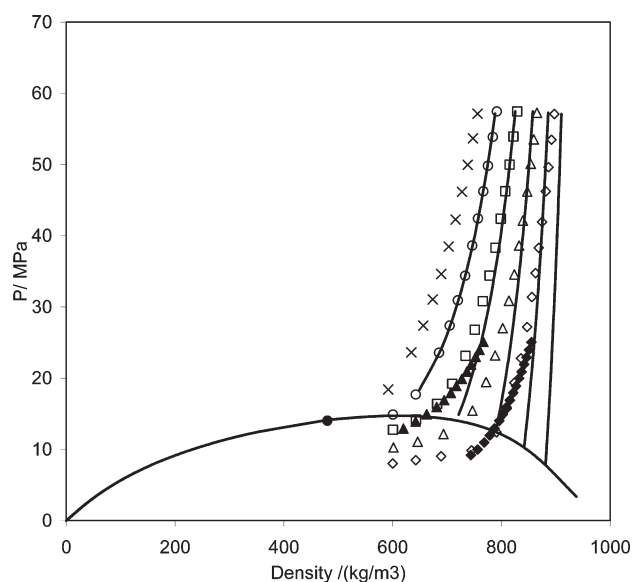


**Figure 11.** Phase equilibrium diagram (pressure–density) at constant composition  $X_1 = 0.5114$  (experimental data<sup>28</sup>) and at constant composition  $X_1 = 0.5569$  (experimental data<sup>29</sup>) for the carbon dioxide (1) + ethanol (2) system. Experimental data:<sup>28</sup>  $\diamond$ ,  $T = 323$  K;  $\triangle$ ,  $T = 348$  K;  $\square$ ,  $T = 373$  K;  $\circ$ ,  $T = 398$  K;  $\times$ ,  $T = 423$  K. Experimental data:<sup>29</sup>  $\blacksquare$ ,  $T = 323$  K;  $\blacktriangle$ ,  $T = 342$  K. Calculation:  $\bullet$ , predicted critical point; —, GEOS/2PCMR prediction.

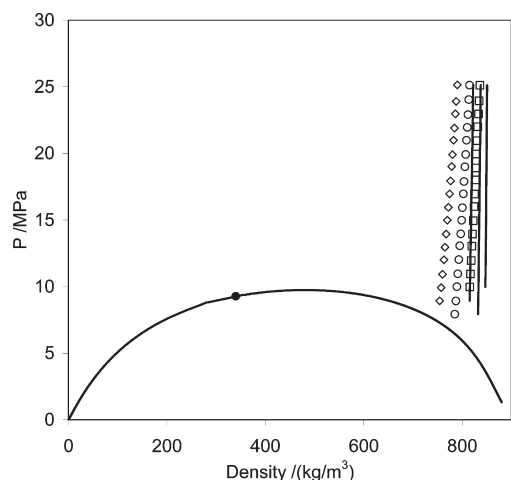


**Figure 12.** Phase equilibrium diagram (pressure–density) at constant composition ( $X_1 = 0.2317$ ) for the carbon dioxide (1) + ethanol (2) system. Experimental data:<sup>29</sup>  $\square$ ,  $T = 312.95$  K;  $\circ$ ,  $T = 332.79$  K;  $\diamond$ ,  $T = 352.67$  K. Calculation:  $\bullet$ , predicted critical point; —, GEOS/2PCMR prediction.

Due to the fact that GEOS reproduce well the volumetric behavior of pure components, the isotherms of the mixtures rich in carbon dioxide or ethanol are also well-predicted (see the deviations in Table 4 for the compositions 0.90404, 0.80722, 0.70951, and 0.23170). The predictions obtained for the mixtures with compositions 0.51143 and 0.40760 are in satisfactory agreement with the experimental data.

At high pressures a better agreement between the predicted densities and the measured data is observed. In the range of lower pressures, near the phase boundary line, the deviations of the

prediction results compared to experimental data are higher. Moreover, in this pressure range the experimental isotherms cross over the phase boundary line predicted by GEOS, several points being in the two-phase region. Unfortunately, there are no available data on the phase boundary line to confirm the GEOS prediction of this curve. It is possible that the GEOS equation predicts higher bubble-point pressures for the mixture carbon dioxide + ethanol. We have not observed this behavior for refrigerant mixtures (see Figure 8 in our previous paper<sup>8</sup>).

The measured densities of Zuniga-Moreno and Galicia-Luna<sup>29</sup> are situated at lower pressures in comparison with the data of Pohler and Kiran<sup>28</sup> (see Figure 11), and consequently deviations in predicted results are higher for the data of Zuniga-Moreno and Galicia-Luna. This is the reason for the AAD of 14.4 % in Table 4 for the GEOS predictions for these experimental data. On the other hand, the large deviation between experimental data and calculations (Figure 12) are only apparent, the average deviations in Table 4 being 4.7 %. The steep increase in pressure with changes in the density mentioned for pure ethanol is also observed in this rich ethanol mixture.

## CONCLUSIONS

In this work we made new measurements with a static-analytical method using a ROLSI,<sup>4</sup> in a high-pressure visual cell with variable volume, for carbon dioxide + ethanol at (333.2, 343.2, 363.2, and 373.2) K and pressures between (1.1 and 14.1) MPa. New critical points (pressure–temperature–composition) were measured in the same visual cell at pressures between (9.1 and 13.9) MPa. Due to the ROLSI coupled to a GC for analysis used in this work, the new measured data sets are of better quality than those previously reported in the literature.

Measured VLE data and literature data for carbon dioxide + ethanol system were modeled with a general cubic equation of state (GEOS) using classical van der Waals (two-parameter conventional mixing rule, 2PCMR) mixing rules.

A single set of interaction parameters, representing the CPM well, was used in this work to represent the new VLE data and critical points and to predict the densities of the mixtures in a wide range of temperature, pressure, and composition. The predicted results were compared to the new data reported in this work and to available literature density data. The predictions show a satisfactory agreement between the model and the experimental data.

## AUTHOR INFORMATION

### Corresponding Author

\*Tel.: +4021 4023988. Fax: +4021 3154193. E-mail address: v\_feriu@chim.upb.ro.

### Funding Sources

The work has been funded by the Sectoral Operational Programme Human Resources Development 2007–2013 of the Romanian Ministry of Labour, Family and Social Protection through the Financial Agreement POSDRU/88/1.5/S/61178.

## REFERENCES

- (1) Stievano, M.; Elvassore, N. High-pressure density and vapor–liquid equilibrium for the binary systems carbon dioxide–ethanol, carbon dioxide–acetone and carbon dioxide–dichloromethane. *J. Supercrit. Fluids* **2005**, *33*, 7–14.



- (2) Christov, M.; Dohrn, R. High-pressure fluid phase equilibria: experimental methods and systems investigated (1994–1999). *Fluid Phase Equilib.* **2002**, *202*, 153–218.
- (3) Secuianu, C.; Feroiu, V.; Geana, D. Phase behavior for carbon dioxide + ethanol system: Experimental measurements and modeling with a cubic equation of state. *J. Supercrit. Fluids* **2008**, *47*, 109–116.
- (4) Guilbot, P.; Valtz, A.; Legendre, H.; Richon, D. Rapid on-line sampler-injector: a reliable tool for HT-HP sampling and on-line GC analysis. *Analisis* **2000**, *28*, 426–431.
- (5) Geana, D. A new equation of state for fluids. I. Applications to PVT calculations for pure fluids. *Rev. Chim. (Bucharest)* **1986**, *37*, 303–309 (in Romanian).
- (6) Geana, D. A new equation of state for fluids. II. Applications to phase equilibria. *Rev. Chim. (Bucharest)* **1986**, *37*, 951–959 (in Romanian).
- (7) Geana, D.; Feroiu, V. Thermodynamic properties of pure fluids using the GEOS3C equation of state. *Fluid Phase Equilib.* **2000**, *174*, 51–68.
- (8) Feroiu, V.; Geana, D. Volumetric and thermodynamic properties for pure refrigerants and refrigerant mixtures from cubic equations of state. *Fluid Phase Equilib.* **2003**, *207*, 283–300.
- (9) Secuianu, C.; Feroiu, V.; Geana, D. High-pressure vapor–liquid equilibria in the system carbon dioxide and 2-propanol at temperatures from 293.25 K to 323.15 K. *J. Chem. Eng. Data* **2003**, *48*, 1384–1386.
- (10) Secuianu, C.; Feroiu, V.; Geana, D. High-pressure phase equilibria for the carbon dioxide + methanol and carbon dioxide + isopropanol systems. *Rev. Chim. (Bucharest)* **2003**, *54*, 874–879.
- (11) Secuianu, C.; Feroiu, V.; Geana, D. High-pressure vapor–liquid equilibria in the system carbon dioxide + 1-butanol at temperatures from (293.15 to 324.15) K. *J. Chem. Eng. Data* **2004**, *49*, 1635–1638.
- (12) Secuianu, C.; Feroiu, V.; Geana, D. Investigation of phase equilibria in the ternary system carbon dioxide + 1-heptanol + n-pentadecane. *Fluid Phase Equilib.* **2007**, *261*, 337–342.
- (13) Secuianu, C.; Feroiu, V.; Geana, D. High-pressure phase equilibria in the (carbon dioxide + 1-hexanol) system. *J. Chem. Thermodyn.* **2010**, *42*, 1286–1291.
- (14) Secuianu, C.; Feroiu, V.; Geana, D. Phase equilibria of carbon dioxide + 1-nonanol system at high pressures. *J. Supercrit. Fluids* **2010**, *55*, 653–661.
- (15) Secuianu, C.; Feroiu, V.; Geana, D. Phase behavior for the carbon dioxide + N-pentadecane binary system. *J. Chem. Eng. Data* **2010**, *55*, 4255–4259.
- (16) Scheidgen, A. Fluidphasengleichgewichte binärer und ternärer Kohlendioxidmischungen mit schwerflüchtigen organischen Substanzen bis 100 MPa. Cosolvency effect und Miscibility windows. Ph.D. Thesis, Ruhr-Universität Bochum, Bochum, Germany, 1997.
- (17) Reid, R. C.; Prausnitz, J. M.; Poling, B. E. *The properties of gases and liquids*, 4th ed.; McGraw-Hill: New York, 1988; Appendix A.
- (18) van Konynenburg, P. H.; Scott, R. L. Critical lines and phase equilibria in binary van der Waals mixtures. *Philos. Trans. R. Soc. London, Ser. A* **1980**, *298*, 495–540.
- (19) Polishuk, I.; Wisniak, J.; Segura, H.; Yelash, L. V.; Kraska, T. Prediction of the critical locus in binary mixtures using equation of state II. Investigation of van der Waals-type and Carnahan–Starling-type equations of state. *Fluid Phase Equilib.* **2000**, *172*, 1–26.
- (20) Geana, D.; Rus, L. Phase equilibria database and calculation program for pure components systems and mixtures. *Proc. Romanian Int. Conf. Chem. Chem. Eng. (RICCCE XIV), Bucharest, Romania* **2005**, *2*, 170–178.
- (21) Heidemann, R. A.; Khalil, A. M. The calculation of critical points. *AIChE J.* **1980**, *26*, 769–779.
- (22) Stockfleth, R.; Dohrn, R. An algorithm for calculating critical points in multicomponent mixtures which can easily be implemented in existing programs to calculate phase equilibria. *Fluid Phase Equilib.* **1998**, *145*, 43–52.
- (23) Lim, J. S.; Lee, Y.-W.; Kim, J.-D.; Lee, Y. Y.; Chun, P.-S. Mass-transfer and hydraulic characteristics in spray and packed extraction columns for supercritical carbon dioxide–ethanol–water system. *J. Supercrit. Fluids* **1995**, *8*, 127–137.
- (24) Galicia-Luna, L. A.; Ortega-Rodriguez, A.; Richon, D. New apparatus for the fast determination of high-pressure vapor–liquid equilibria of mixtures and of accurate critical pressures. *J. Chem. Eng. Data* **2000**, *45*, 265–271.
- (25) Ziegler, J. W.; Chester, T. L.; Innis, D. P.; Page, S. B.; Dorsey, J. G. Supercritical fluid flow injection method for mapping liquid–vapor critical loci of binary mixtures containing CO<sub>2</sub>. In *Innovations in Supercritical Fluids, Science and Technology*; ACS Symposium Series, Vol. 608; Hutchenson, E. K. H., Foster, N. R., Eds.; American Chemical Society: Washington, DC, 1995; pp 93–110.
- (26) Joung, S. N.; Yoo, C. W.; Shin, H. Y.; Kim, S. Y.; Yoo, K.-P.; Lee, C. S.; Huh, W. S. Measurements and correlation of high-pressure VLE of binary CO<sub>2</sub>–alcohol systems (methanol, ethanol, 2-methoxyethanol and 2-ethoxyethanol). *Fluid Phase Equilib.* **2001**, *185*, 219–230.
- (27) Li, C. C. Critical temperature estimation of simple mixtures. *Can. J. Chem. Eng.* **1971**, *49*, 709–710.
- (28) Pohler, H.; Kiran, E. Volumetric properties of carbon dioxide + ethanol at high pressures. *J. Chem. Eng. Data* **1997**, *42*, 384–388.
- (29) Zuniga-Moreno, A.; Galicia-Luna, L. A. Compressed Liquid Densities of Carbon Dioxide + Ethanol Mixtures at Four Compositions via a Vibrating Tube Densimeter up to 363 K and 25 MPa. *J. Chem. Eng. Data* **2002**, *47*, 149–154.